

# Dalton Transactions

Accepted Manuscript



This is an *Accepted Manuscript*, which has been through the Royal Society of Chemistry peer review process and has been accepted for publication.

*Accepted Manuscripts* are published online shortly after acceptance, before technical editing, formatting and proof reading. Using this free service, authors can make their results available to the community, in citable form, before we publish the edited article. We will replace this *Accepted Manuscript* with the edited and formatted *Advance Article* as soon as it is available.

You can find more information about *Accepted Manuscripts* in the [Information for Authors](#).

Please note that technical editing may introduce minor changes to the text and/or graphics, which may alter content. The journal's standard [Terms & Conditions](#) and the [Ethical guidelines](#) still apply. In no event shall the Royal Society of Chemistry be held responsible for any errors or omissions in this *Accepted Manuscript* or any consequences arising from the use of any information it contains.

# Structural Diversity of Lamellar Zeolite Nu-6(1) — Postsynthesis of Delaminated Analogues

Hao Xu, Lili Jia, Haihong Wu,\* Boting Yang, Peng Wu\*

*Shanghai Key Laboratory of Green Chemistry and Chemical Processes, Department of Chemistry, East China Normal University, North Zhongshan Road 3663, Shanghai 200062, China*

*\*Corresponding authors. Tel/Fax: +86-21 62232292; [pwu@chem.ecnu.edu.cn](mailto:pwu@chem.ecnu.edu.cn);*

*[hhwu@chem.ecnu.edu.cn](mailto:hhwu@chem.ecnu.edu.cn)*

## Abstract

Nu-6(1) zeolite, the lamellar precursor of NSI topology, was firstly synthesized with 4'4-bipyridine as the structure-directing agent (SDA) and then subjected to HCl/EtOH treatment for the purpose of structural modification. Interlayer deconstruction and reconstruction took place alternately in this acid treatment. An intermediate named ECNU-4 was separated at initial stage of this continuous treatment process, which exhibited a special X-ray diffraction pattern without obvious reflection peaks at low degree. The zeolitic structure in intralayer sheets was supposed to be well preserved in ECNU-4, whereas the interlayer structure became extremely disordered. The ECNU-4 intermediate showed a structural diversity. It was converted into the reconstructed and interlayer expanded zeolite IEZ-NSI without external silicon source, by prolonging the treatment time of HCl/EtOH to 24 h. Moreover, with a partially delaminated structure, ECNU-4 was easily interlayer swollen at room temperature with cetyltrimethyl ammonium bromide in the presence of tetrapropyl ammonium hydroxide. The swollen material was further sonicated to yield a more deeply delaminated zeolite Del-Nu-6. ECNU-4 and Del-Nu-6 differed in delamination degree, structural disordering and textural properties especially surface area.

## Keywords

Layered zeolite, Nu-6(1), delamination, deconstruction, reconstruction

## Introduction

Zeolites constructed by  $\text{SiO}_4$  and/or  $\text{AlO}_4$  tetrahedrons exhibit crystalline and rigid 3-dimensional (3D) structures<sup>1</sup> which are hardly changed by post-treatments like calcination, dealumination and desilication.<sup>2</sup> Different from conventional ones, a class of zeolites originate from layered precursors that are of 2D structures and consist of discrete crystalline layers, between which are structure-directing agents.<sup>3</sup> Up to date, those so-called lamellar zeolites account more than 20 kinds,<sup>4-6</sup> including the traditional MCM-22(P),<sup>7</sup> Nu-6(1),<sup>8</sup> PREFER<sup>9</sup> and the newly found layered MFI zeolite<sup>10</sup> and IPC-1P.<sup>11</sup> The layer surface of lamellar zeolites is terminated by silanols, which form linkage between neighboring layers through weak hydrogen bonds or SDA molecules. It is the interlayer weak hydrogen bonds that make possible the tailoring of the interlayer linkage, and endow lamellar zeolites with structural diversity as well.

Five kinds of modification methods have been developed to tailor the linkage during the past two decades with the purpose to increase the interlayer space or external surface area, including swelling,<sup>12</sup> pillaring,<sup>12</sup> delamination,<sup>13</sup> interlayer silylation<sup>14</sup> and detemplating.<sup>15,16</sup> Swelling treatment is carried out in the alkaline solution and in the presence of surfactant molecules. The surface silanols would deprotonate in the alkaline medium forming  $\text{SiO}^-$  groups and thus repulse with each other, which then provide enough space for the intercalation of surfactant molecules.<sup>12,17</sup> The interlayer space can be enlarged to ca. 3 nm contributed by double

layer surfactant molecules. Delaminated material, with “house-of-cards” topology and disorder collection of single layers,<sup>13</sup> is obtained by performing an ultrasound treatment on the swollen material. Single sheet with one or less unit cell can be found in the delaminated material, exhibiting extremely large external surface area compared to its corresponding 3D structure, such as ITQ-2 exhibiting surface area (BET) of  $\geq 700 \text{ m}^2 \text{ g}^{-1}$ .<sup>13,18,19</sup> Apart from full delamination, partially delaminated materials, such as MCM-56, can be obtained by direct synthesis<sup>20</sup> or mild acid treatment on the as-made layered zeolite MCM-22(P).<sup>16,21</sup> In a typical pillaring process, polymerized tetraethyl orthosilicate (TEOS) are introduced into the interlayer space of swollen materials to serve as pillars, inducing mesopores between neighboring layers.<sup>12,22-24</sup> In contrast to pillaring process, specially chosen monomeric silanes with two inactive groups and active groups attached to silicon atoms are used in the silylation process.<sup>14,25-28</sup> Thus, mono silane molecules serve as props to connect the up-and-down layers, leading to newly formed and enlarged interlayer pore channels. Silylation process can be carried out on both as-made layered zeolite and swollen materials, depending on the interlayer space and the size of silane molecules.<sup>29,30</sup> These modified layered zeolites showed higher activity than their corresponding 3D type zeolite in acid catalyzed reactions<sup>31,32</sup> or liquid phase oxidation reactions,<sup>19,25,33</sup> because the increased pore size or enlarged external surface area favored the diffusion of substrates and the accessibility to active sites.

Discoveries of new layered zeolites were rare and accidental while Ryoo<sup>10</sup> demonstrated remarkable deliberate preparation using specially designed SDA with

one side directing the crystallization of zeolitic layers and the other side interrupting the interlayer continuous growth. This method has also been expanded to synthesis other lamellar zeolites such as layered MTW zeolite. On the other hand, Roth et al. reported a selective deconstruction of the UTL germanosilicate with 3D crystalline structure, yielding a novel layered zeolite IPC-1P.<sup>11</sup> The existence of interlayer less stable Ge-rich double 4-ring (D4R) units is the premise of such structural hydrolysis. Then the layered zeolite can be reconstructed to two new IPC-2 and IPC-4 zeolites through silylation and calcination.<sup>34</sup> More layered zeolites are expected to emerge after developing new synthesis methods.

3D NSI zeolite, coming from corresponding Nu-6(1) lamellar precursor, possesses strong acid sites and shows potentiality in the acid catalyzed reactions<sup>35</sup> and separation as membrane.<sup>36</sup> However, the pore sizes of its two sets of screwy 8-membered ring (MR) channels are relatively small, which induces severe diffusion constrains over the substrates.<sup>35</sup> Previous researches have concentrated on the swelling and delaminating of the Nu-6(1) zeolite,<sup>37-40</sup> with the expectation of increasing the external surface area. Nevertheless, the swelling process is not easy for Nu-6(1). A successful swelling can only be realized with the small-size decyltrimethylammonium (DTA<sup>+</sup>) ions<sup>37</sup> or pre-treatment of acid washing.<sup>40</sup> Moreover, the Si/Al ratio<sup>41</sup> of Nu-6(1) zeolite also has effect on the delamination process.<sup>39</sup> With a screwy pore structure, Nu-6(1) zeolite showed unusual phenomena in the post-treatments. Thus, it is desirable to find new routes to open the porosity of NSI zeolite. We recently reported the interlayer expansion of Nu-6(1) with an improved silylation method.<sup>42</sup>

Although water is usually employed as the solvent for silylating many zeolite precursors, using ethanol as the solvent exhibited superiority in silylating Nu-6(1). In ethanol, the extraction of organic SDA species and the insertion of silane molecules matched well with each other, inducing a more ordered interlayer expanded structure with double 10 MR pore channels. With larger interlayer space, the IEZ-Nu-6(1) zeolite showed a higher activity than the 3D NSI zeolite, i.e. Nu-6(2), in the esterification of acetic acid and ethanol.

In this study, we have traced in detail the acid treatment process of Nu-6(1) in ethanol but in the absence of any silane. A continuous interlayer structural deconstruction and reconstruction occurred, and the removable silicon species were finally inserted between the layers to obtain IEZ-NSI. The product with an interlayer collapsed structure at initial treatment stage was separated and its structural properties were investigated by comparing to those of Nu-6(2). Moreover, the material was further subjected to swelling and delamination under mild conditions.

## Experimental

### *Chemicals and materials*

4,4'-Bipyridine and dimethyldiethoxysilane were purchased from Tokyo Chemical Industry Co., Ltd (TCI). H<sub>2</sub>SO<sub>4</sub> (98 wt.%) and HCl (36 wt.%) were purchased from Shanghai Chemical Reagent Co., Ltd. Ethanol and cetyltrimethylammonium bromide were purchased from Shanghai Shangsi Refine Chemical Industrial Co., Ltd. Aluminum sulfate octadecahydrate was purchased from Sinopharm Chemical Reagent Co., Ltd. Tetrapropylammonium hydroxide was purchased from ACORS Organics.

Sodium silicate (27.099% SiO<sub>2</sub>, 8.693% Na<sub>2</sub>O) was obtained from industry. All of these chemicals were used without further purification.

### *Synthesis of Nu-6(1) lamellar precursor*

The lamellar precursor Nu-6(1) zeolite was synthesized using 4'4'-bipyridine as the structure directing agent (SDA) according to literature method.<sup>37</sup> In a typical synthesis, the following A, B and C solutions were prepared separately. Solution A was obtained by dissolving 1.82 g 4'4'-bipyridine in 10.08 g ethanol. 18.45 g sodium silicate (27.099% SiO<sub>2</sub>, 8.693% Na<sub>2</sub>O) was diluted with 14.92 g H<sub>2</sub>O forming solution B. Solution C was prepared by dissolving 0.62 g aluminum sulfate octadecahydrate and 1.52 g sulfuric acid in 22.78 g H<sub>2</sub>O. Then, solution B and C were added dropwise into solution A under stirring, forming finally a homogeneous synthetic gel with a Si/Al ratio of 45. The gel was transferred into a Teflon-lined stainless steel autoclave (120 mL), and was crystallized under tumbling at 408 K for 3 days. The resulting product was filtered off, washed with distilled water and dried at 353 K overnight, yielding 5.2 g Nu-6(1) precursor. Direct calcination of Nu-6(1) zeolite at 823 K for 6 h induced a structural condensation forming 3D NSI type zeolite.

### *Postsynthesis of ECNU-4 material*

1.0 g as-made Nu-6(1) zeolite was treated with 50 mL HCl (2 M) in ethanol solution at 473 K for different time (15 min - 24 h). The partially delaminated analogue, denoted as ECNU-4, was obtained at 30 min of HCl/EtOH treatment (yield, 90 wt.%). It was then calcined at 823 K for 6 h yielding ECNU-4-Cal zeolite. Prolonging the HCl/EtOH treatment to 24 h, an interlayer expanded zeolite was

obtained, denoted as IEZ-Nu-6(1). For control experiment, interlayer expanded Nu-6(1) was also prepared by silylation technique. Nu-6(1) was silylated with  $\text{Me}_2\text{Si}(\text{OEt})_2$  (DEDMS) silane in 2 M HCl/EtOH solution using 0.08 g silane per gram of Nu-6(1) precursor.<sup>42</sup> After carrying out the silylation with silane at 473 K for 24 h, the product denoted as IEZ-Nu-6(1)-Si was obtained.

### *Swelling and delamination of ECNU-4*

ECNU-4 was swollen in the mixture of tetrapropylammonium hydroxide (TPAOH) and cetyltrimethylammonium bromide (CTAB) at room temperature under vigorous stirring.<sup>17</sup> In a typical run, 1.0 g ECNU-4 and 5.8 g CTAB were dissolved in 15.6 g  $\text{H}_2\text{O}$ . Then, a desirable amount of TPAOH (25 wt.%) (1.5 – 3.6 g) was added into the solution. After the treatment for 10 h, the final product was collected by centrifugation, washed with distilled water and dried at 353 K overnight. It was denoted as swollen ECNU-4 ( $x$ ), where  $x$  represents the amount of TPAOH used. To prepare a delaminated material, the swollen mixture was subjected to an ultrasonic treatment (50 W, 40 KHz) for 1 h. The resulting product was collected by centrifugation and further calcined 823 K for 6 h to remove the occluded organic species, giving rise to delaminated material, Del-Nu-6-( $x$ ), where  $x$  means the amount of TPAOH added in the swelling mixture. For comparison, Nu-6(1) precursor was swollen directly using the same procedure.

### *Characterization methods*

Powder X-ray diffraction (XRD) patterns were collected on a Rigaku Ultima IV X-ray diffractometer using  $\text{CuK}_\alpha$  radiation ( $\lambda = 1.5405 \text{ \AA}$ ). Nitrogen adsorption

isotherms were recorded at 77 K on a BELSORP-MAX instrument after activating the calcined samples at 573 K or the dried samples at 393 K under vacuum for at least 10 h. The SEM images were taken on a Hitachi S-4800 microscope. The Si/Al ratio was measured with inductively coupled plasma (ICP) spectroscopy on a Thermo IRIS Intrepid II XSP atomic emission spectrometer. Zeolites were dissolved in the HF solution in advance. The thermogravimetric and differential thermal analyses (TG-DTA) were performed on a Mettler–Toledo Model TGA/SDTA851e apparatus from room temperature to 1073 K at a heating rate of 10 K min<sup>-1</sup> in air. <sup>29</sup>SiMAS NMR spectra were recorded on a Varian ModelVNMRS-400WB spectrometer under one pulse condition and cross-polarization, respectively. <sup>29</sup>Si NMR spectra were acquired with a 7.5mm T3HX probe at 79.43 MHz and a spinning rate of 3 kHz. The chemical shift was referred to 2,2-dimethyl-2-silapentane-5-sulfonic acid sodium salt ((CH<sub>3</sub>)<sub>3</sub>Si(CH<sub>2</sub>)<sub>3</sub>SO<sub>3</sub>Na).

## Results and discussion

Nu-6(1) lamellar precursor and its calcined derivate Nu-6(2) were firstly reported by Whittam in the early 1980s.<sup>8</sup> Although the layer structure is very similar with those of MCM-69<sup>43</sup> and EU-19<sup>44</sup> zeolites, Nu-6(1) possesses a different symmetry of P2<sub>1</sub>/a because of the large-sized 4'4-bipyridine molecules intercalating the layers.<sup>35</sup> The calcination treatment on the as-made Nu-6(1) precursor led to the decomposition of SDA molecules and simultaneous condensation of the up-and-down layers. As shown in Figure 1a and b, the layer-related 200 reflection peak shifted largely from 6.5° to

10.4° upon calcination. In addition, the resultant product, Nu-6(2) with the NSI topology, showed an XRD pattern with lower intensities and broader peaks than that of Nu-6(1), implying a structural disordering occurred slightly during the calcination process. The Nu-6(2) zeolite possesses two sets of channels restricted by severely twisted 8 MR pore windows, the sizes of which are thus relatively small.<sup>35</sup> To enlarge the pore entrance, interlayer expansion was performed in an acidic medium with or without silane silylation (Figure 1 c and d). After silylation, the 200 reflection peak emerged at a lower angle than that of Nu-6(2), which is indicative of an enlarged interlayer space. The silylation constructed new 10 MR channels with two additional Si atoms inserted between the layers,<sup>42</sup> while the Nu-6(2) zeolite is of 8 MR pore structure.<sup>35</sup> Although the interlayer expansion can be realized without additional Si source, the quality of XRD pattern of IEZ-Nu-6(1) was poorer than that of IEZ-Nu-6(1)-Si prepared with silane (Figure 1c and 1d). Additionally added Si source favored the formation of more ordered interlayer expanded structure. However, the amount of silica source should be well controlled to avoid self-condensation and then formation of amorphous phase.<sup>42</sup>

Ethanol other than usually used water was employed as the solvent because in ethanol the SDA molecules were extracted more slowly, which has been disclosed in our previous research.<sup>42</sup> The SDA extraction process in the HCl/EtOH system without silane was also investigated. TG curves of as-made Nu-6(1) precursor and its acid-treated materials with different time were measured (Figure 2a-h). Three distinguished steps were observed in the TG curves of Nu-6(1) zeolite. The first step

of ca. 3 wt.% weight loss was in the region of 25 - 300 °C, followed by a large weight loss of 15 wt.% in the region of 300 - 390 °C. The additional weight loss of ca. 6 wt.% occurred in the region > 400 °C. The total weight loss of as-made Nu-6(1) was about 24 wt.%, which was consistent with the value reported in the literature.<sup>39</sup> The weight loss in the low temperature region is attributed to the physically adsorbed water molecules while that in the higher temperature region is due to the decomposition of organic SDA molecules.<sup>38</sup> The condensation and dehydration of interlayer silanols may also contribute to the weight loss in the higher temperature region. After the acid treatment in the HCl/EtOH system, the SDA molecules were more or less extracted depending on the treatment time. Subtracting the physically adsorbed water in low-temperature region, the weight loss contributed by SDA molecules were calculated according to the TG curves and they were shown against the treatment time in Figure 2i. The content of remaining SDA kept decreasing during the first 2.5 h. However, an increase was observed at 4 h and then the curve came to level off in the last 20 hours.

The structural changes during HCl/EtOH treatment were also traced by XRD investigation (Figure 3). The intensity of reflection peaks especially those attributed to 200 and 002 planes largely decreased during the first 15 min with only very weak and broad peaks can be observed (Figure 3a). The peak intensity became even weaker in the next 15 minutes with the 200 reflection peak disappearing at 30 min (Figure 3b and 3c). The disappearance of 200 reflection peak and extremely weak 002 peak meaning the disorder stacking style of the NSI layers and the deconstruction of

original interlayer connection. The 200 reflection peak appeared again when the treatment time was increased to 75 min, but shifted to higher angle of  $2\theta = 7.8^\circ$  compared with the as-made Nu-6(1) zeolite (Figure 3d). After that, the reflections were gradually intensified with prolonging the acid treatment time. Meanwhile, the 200 reflection shifted slightly to lower angles while the structure was reconstructed (Figure 3e-g). The material obtained at 24 h of acid treatment was exactly the interlayer-expanded and reconstructed structure IEZ-Nu-6(1). Based on the above results, the reconstruction is deduced to take place by the silylation with the silica debris washed out of the zeolite crystals. This phenomenon has been actually observed in the acid treatment of other zeolite precursors like Ti-MWW<sup>45</sup> and PLS-*n* series.<sup>46</sup>

During HCl/EtOH treatment, Nu-6(1) zeolite underwent an interlayer deconstruction and reconstruction process, indicated by the dramatic changes of 200 and 002 diffraction peaks. It should be noted that the structural deconstruction and reconstruction only happened in the interlayer space and don't mean a whole structural collapse and recrystallization. In the deconstruction step, 43% of organic SDA molecules were removed from the Nu-6(1) precursor by the acid treatment for 30 min. With prolonging the acid treatment time, the removable silica species eluted from the crystals diffused into the interlayer space and reacted with the silanol groups, forming new Si-O-Si linkages. During the reconstruction process, the SDA content firstly decreased and then increased slightly (Figure 2i). The reconstruction of the interlayer pore channels may cause some SDA molecules in the solvent to be

reinserted into the newly formed 10 MR pores. Apart from this interesting deconstruction and reconstruction phenomenon, the interlayer collapsed structure obtained at 30 min also aroused our interest. It was separated from the above seven acid-treated derivatives, denoted as ECNU-4. The XRD patterns of ECNU-4 before and after calcination are shown in the Figure 4. The structure became more disordered upon calcination treatment with the intensity of peaks in higher degrees becoming weaker. From the XRD patterns, ECNU-4 seems to be deconstructed materials if compared with Nu-6(1) and Nu-6(2) both having well-resolved reflections (Figure 4a and 4d).

As ECNU-4 was readily converted to interlayer-expanded Nu-(6) when the HCl/EtOH treatment time was prolonged over 2.5 h (Figure 3), it is presumed to be still composed of the collection of NSI sheets or layers but without ordered stacking. The extraction of SDA molecules, that is, the interlayer pillars could be responsible for the disturbing of layer stacking and the weak reflections observed in XRD patterns of ECNU-4. Similar result has already been obtained for MCM-22(P). A mild acid treatment over MCM-22(P) produced the partially delaminated material MCM-56 analogue.<sup>16,21</sup> In fact, the XRD pattern of ECNU-4 was very similar with that of calcined MCM-39 zeolite.<sup>40</sup> MCM-39 zeolite was prepared by treating Nu-6(1) with 2 M HCl aqueous solution at relatively low temperature of 363 K for three times. MCM-39 showed very sharp reflections, indicative of a well-defined structure.<sup>40</sup> However, its reflection peaks became weak and broad upon calcination, indicating structure disordering occurred as a result of interlayer condensation. Compared with

ECNU-4, the calcined MCM-39 possesses two additional weak reflections in the  $2\theta$  region of  $10-15^\circ$ , suggesting it possesses higher structure order. Both calcined MCM-39 and ECNU-4 can be viewed as delaminated materials, although the preparation methods and the degrees of structural disorder are different.

ITQ-18 is a fully delaminated material of Nu-6(1).<sup>37</sup> It was prepared by the combination of preswelling and ultrasound treatment. Layered zeolites are usually swollen in a mixture of TPAOH and CTAB at 353 K. However, Nu-6(1) zeolite cannot be efficiently swollen using CTAB surfactant molecules. Although Zubowa et al.<sup>38</sup> increased the treatment time and temperature, a fully swelling was not achieved either with CTAB. A smaller-sized surfactant decyltrimethylammonium bromide (DTAB) then was used to realize a fully swelling.<sup>37</sup> We have also attempted to swell Nu-6(1) in this study. Different from traditional swelling process, the delaminated material ECNU-4 was employed as the starting material for swelling. To avoid the desilication of layer structure in the alkaline solution at high temperature, swelling process was carried out at room temperature. Figure 5A showed the XRD patterns of swollen ECNU-4 with different amount of TPAOH. After swelling, a new peak appeared at  $2\theta=3^\circ$  with an interlayer distance around 2.94 nm, indicating a successful interlayer intercalation by CTAB molecules. There is no obvious difference over these swollen materials prepared with different amount of TPAOH. However, some of the layers were not expanded by the CTAB molecules because of the weak reflection corresponding to the layer structure in original Nu-6(1) still existed at around  $6.5^\circ$ . In control experiment, the direct swelling was attempted on the Nu-6(1) precursor at

room temperature. However, no swollen refraction was observed in the XRD pattern (Figure S1). This means that the partially delaminated structure of ECNU-4 favored a mild swelling at room temperature. Then, ultrasound treatment was performed on the swollen ECNU-4 to give rise to Del-Nu-6 (Figure 5B), the XRD pattern of which was very similar with that of ITQ-18 zeolite prepared by a high-temperature swelling.<sup>37</sup>

Alkaline medium is critical for the cleavage of interlayer hydrogen bonds and then the successful swelling of layered zeolites, which is often realized by using TPAOH. It is a dilemma that desilication always happened together with the swelling process in the alkaline aqueous solution. As a result, the amount of TPAOH should be carefully controlled to avoid a severe desilication. Swelling and delamination are aimed to increase the external surface area to increase the accessibility of active sites. N<sub>2</sub> adsorption isotherms of Del-Nu-6 were measured to evaluate the external surface area. As shown in Figure 6, the swelling and delamination made the N<sub>2</sub> adsorption amount increase further when the amount of TPAOH was increased from 1.5 g to 3.6 g. The total surface area determined by BET method was also increased with increasing amount of TPAOH (Table 1). However, the external surface area determined by *t*-plot method reached the highest value of 87 m<sup>2</sup> g<sup>-1</sup> when 2.4 g TPAOH was used. The decrease of the external surface area may be caused by a severe desilication when the amount of TPAOH was larger than 2.4 g. Moreover, the yield decreased from 95% to 84% when increasing the amount of TPAOH, indicating the dissolution at high pH condition. To protect the layer structure and obtain the highest external surface area, the suitable TPAOH amount was set at 2.4 g per gram

of zeolite when performing the swelling process. Although delaminated zeolite of Del-Nu-6 showed much higher surface area than Nu-6(2) zeolite, the value was lower than those reported in the literature ( $300 - 600 \text{ m}^2 \text{ g}^{-1}$ ),<sup>37-39</sup> which may be related with the mild swelling condition obtained in our study.

Two kinds of delaminated materials with different delamination degrees, that is, ECNU-4 and Del-Nu-6, were obtained by combining HCl/EtOH treatment and subsequent surfactant-assisted swelling. As shown in Scheme 1, partially delaminated ECNU-4 was obtained from the Nu-6(1) precursor by the acid treatment for a short treatment time of 30 min. Then ECNU-4 was subjected to mild swelling and delamination at room temperature, yielding more deeply delaminated material of Del-Nu-6. The differences between ECNU-4 and Del-ECNU-4 were carefully studied using  $\text{N}_2$  adsorption, SEM, and  $^{29}\text{Si}$  NMR techniques.

As shown in Figure 6, both of calcined ECNU-4 and Del-Nu-6 had a higher  $\text{N}_2$  adsorption capacity than Nu-6(2) despite the fact that ECNU-4-Cal had a very poor XRD pattern. Compared with ECNU-4, the Del-Nu-6 samples all possessed larger total surface areas as well as external surface areas (Table 1). The increased external surface area of ECNU-4 was due to a partial exposure of delaminated layer surface. As for Del-Nu-6, in addition to more deeply delaminated structure, mesopores created by desilication during swelling process may also contribute to further enlarged surface area.

The crystals of Nu-6(1) appeared to be thin flakes with 2-3  $\mu\text{m}$  diameter and 200 - 300 nm thickness (Figure 7a). These thin flakes formed the aggregates of  $\sim 5 \mu\text{m}$  in

size, in agreement with that reported in the literature.<sup>38</sup> ECNU-4 showed the same morphology as Nu-6(1) (Figure 7b), indicating the structural changes during acid treatment took place at an atomic level. However, these aggregates were broken up to scattered flakes after swelling treatment in TPAOH (Figure 7c). In addition, the surface and the corner of the crystals have been worn slightly because of desilication even though the swelling was carried out at room temperature. The following ultrasound treatment played no influence on the crystal morphology (Figure 7d). Comparing the SEM images of ECNU-4 and Del-Nu-6(2.4), the delamination by short-time HCl/EtOH treatment made the crystal morphology of the pristine zeolite almost intact, while the TPAOH-assisted delamination caused a part of zeolite crystals deteriorate as a result of the desilication in alkaline medium.

Figure 8 shows the <sup>29</sup>Si MAS NMR spectra of Nu-6(1), Nu-6(2) and the two calcined delaminated materials. Nu-6(1) showed two well-resolved distinct resonances with one located at -103 ppm attributed to Si(OSi)<sub>3</sub>(OH) groups(Q<sup>3</sup>) and the other one attributed the Si(OSi)<sub>4</sub> groups (Q<sup>4</sup>).<sup>39</sup> This lamellar precursor contained 27.68% Q<sup>3</sup> groups as shown in Table 2. Upon calcination, the SDA molecules are removed and the interlayer silanol groups on the layer surface would condensate with each other, producing a 3D-type Nu-6(2) zeolite. The intensity of the Q<sup>3</sup> resonance was thus decreased after calcinations as the transformation to Q<sup>4</sup> groups occurred with the condensation of silanols. However, Nu-6(2) also contained a certain amount of Q<sup>3</sup> groups, which may be attributed to those silanols located on the outer surface and unreacted ones because of the structural disordering during calcination. Both of the

two delaminated materials showed a broad band in region of -100 to -120 ppm (Figure 8c and 8d). The  $^{29}\text{Si}$  MAS NMR spectra can be deconvoluted into one peak belonging to  $\text{Q}^3$  groups and other three peaks assigned to  $\text{Q}^4$  groups (Figure 2S).<sup>39</sup> As shown in Table 2, ECNU-4-Cal and Del-Nu-6(2.4)-Cal contained comparable  $\text{Q}^3$  groups with a proportion around 24 %, much larger than that in Nu-6(2) zeolite. Considering the preparation process of ECNU-4 and Del-Nu-6, the  $\text{Q}^3$  groups in ECNU-4 were mainly contributed by those located on the exposed surface because of the delaminated structure. However, the  $\text{Q}^3$  groups may also come from the desilication of layer structure for Del-Nu-6.

## Conclusions

The interlayer expansion of NSI zeolite can be realized by treating Nu-6(1) precursor in HCl/EtOH solution even without additional silane source, during which a continuous interlayer structural deconstruction and reconstruction takes place in turn. The intermediate ECNU-4 with a greatly disturbed layer arrangement can be obtained by treating Nu-6(1) with HCl/EtOH for 30 min. With very weak XRD reflections, ECNU-4 can be viewed as a partially delaminated analogue, but still possessing well-preserved NSI layers. Starting from ECNU-4, a mild swelling can be realized at room temperature, which is benefit to prepare a more deeply delaminated zeolite Del-Nu-6 without significant crystal dissolving.

## Acknowledgements

We gratefully acknowledge the National Natural Science Foundation of China (21373089, U1162102), Ph. D Programs Foundation of Ministry of Education

(2012007613000), the National Key Technology R&D Program (2012BAE05B02), and the Shanghai Leading Academic Discipline Project (B409).

## Reference

1. R. Xu, W. Pang, J. Yu, Q. Huo, J. Chen, *Chemistry of Zeolites and Related Porous Materials Synthesis and Structure*, Wiley, Singapore, 2007.
2. Y. Tao, H. Kanoh, L. Abrams, K. Kaneko, *Chem. Rev.*, 2006, **106**, 896.
3. W. J. Roth, J. Čejka, *Catal. Sci. Technol.*, 2011, **1**, 43.
4. W. J. Roth, B. Gil, B. Marszalek, *Catal. Today*, 2013, in press.
5. F. S. O. Ramos, M. K. de Pietre, H. O. Pastore, *RSC Adv.*, 2013, **4**, 2084.
6. B. Marler, H. Gies, *Eur. J. Mineral*, 2012, **24**, 405
7. M. E. Leonowicz, J. A. Lawton, S. L. Lawton, M. K. Rubin, *Science*, 1994, **264**, 1910.
8. T. V. Whittam, US patent, 4397825, 1983.
9. L. Schreyeck, P. Caullet, J. C. Mougénel, J. L. Guth, B. Marler, *Micropor. Mater.*, 1996, **6**, 259.
10. M. Choi, K. Na, J. Kim, Y. Sakamoto, O. Terasaki, R. Ryoo, *Nature*, 2009, **461**, 246.
11. W. J. Roth, O. V. Shvets, M. Shamzhy, P. Chlubná, M. Kubů, P. Nachtigall, J. Čejka, *J. Am. Chem. Soc.*, 2011, **133**, 6130.
12. W. J. Roth, C. T. Kresge, J. C. Vartuli, M. E. Leonowicz, A. S. Fung, S. B. McCullen, *Stud. Surf. Sci. Catal.*, 1995, **94**, 301.
13. A. Corma, V. Fornes, S. B. Pergher, Th. L. M. Maesen, J. G. Buglass, *Nature*, 1998, **396**, 353.

14. P. Wu, J. Ruan, L. Wang, L. Wu, Y. Wang, Y. Liu, W. Fan, M. He, O. Terasaki, T. Tatsumi, *J. Am. Chem. Soc.*, 2008, **130**, 8178.
15. A. Burton, R. J. Accardi, R. F. Lobo, M. Falcioni, M. W. Deem, *Chem. Mater.*, 2000, **12**, 2936.
16. L. Wang, Y. Wang, Y. Liu, L. Chen, S. Cheng, G. Gao, M. He, P. Wu, *Micropor. Mesopor. Mater.*, 2008, **113**, 435.
17. S. Maheshwari, E. Jordan, S. Kumar, F. S. Bates, R. L. Penn, D. F. Shantz, M. Tsapatsis, *J. Am. Chem. Soc.*, 2008, **130**, 1507.
18. A. Corma, U. Diaz, M. E. Domine, V. Fornés, *J. Am. Chem. Soc.*, 2000, **122**, 2804.
19. P. Wu, D. Nuntasri, J. Ruan, Y. Liu, M. He, W. Fan, O. Terasaki, T. Tatsumi, *J. Phys. Chem. B*, 2004, **108**, 19126.
20. W. J. Roth, *Stud. Surf. Sci. Catal.*, 2005, **158A**, 19.
21. Y. Wang, Y. Liu, L. Wang, H. Wu, X. Li, M. He, P. Wu, *J. Phys. Chem. C*, 2009, **113**, 18753.
22. S.-Y. Kim, H.-J. Ban, W.-S. Ahn, *Catal. Lett.*, 2007, **113**, 160.
23. A. C. Lara, A. C. Canós, V. F. Seguí, U. D. Morales, US patent, 65550900B1, 2003.
24. P. Chlubná, W. J. Roth, H. F. Greer, W. Zhou, O. Shvets, A. Zúkal, J. Čejka, R. E. Morris, *Chem. Mater.*, 2013, **25**, 542.
25. L. Wang, Y. Wang, Y. Liu, H. Wu, X. Li, M. He, P. Wu, *J. Mater. Chem.*, 2009, **19**, 8594.
26. H. Gies, U. Müller, B. Yilmaz, M. Feyen, T. Tatsumi, H. Imai, H. Zhang, B. Xie, F.-S. Xiao, X. Bao, W. Zhang, T. De Baerdemaeker, D. De Vos, *Chem. Mater.*, 2012,

- 24, 1536.
27. H. Gies, U. Müller, B. Yilmaz, T. Tatsumi, B. Xie, F.-S. Xiao, X. Bao, W. Zhang, D. De Vos, *Chem. Mater.*, 2011, **23**, 2545.
28. H. Xu, B. Yang, J. G. Jiang, L. Jia, M. He, P. Wu, *Micropor. Mesopor. Mater.*, 2013, **169**, 88.
29. A. Corma, U. Díaz, T. García, G. Sastre, A. Velty, *J. Am. Chem. Soc.*, 2010, **132**, 15011.
30. H. Xu, L. Fu, M. He, P. Wu, *Micropor. Mesopor. Mater.*, 2014, in press.
31. B. Yilmaz, U. Müller, M. Feyen, H. Zhang, F.-S. Xiao, T. DeBaerdemaeker, B. Tijsebaert, P. Jacobs, D. De Vos, W. Zhang, X. Bao, H. Imai, T. Tatsumi, H. Gies, *Chem. Commun.*, 2012, **48**, 11549.
32. B. Tijsebaerta, M. Henry, H. Gies, F.-S. Xiao, W. Zhang, X. Bao, H. Imai, T. Tatsumi, U. Müller, B. Yilmaz, P. Jacobs, D. De Vos, *J. Catal.*, 2011, **282**, 47.
33. F.-S. Xiao, B. Xie, H. Zhang, L. Wang, X. Meng, W. Zhang, X. Bao, B. Yilmaz, U. Müller, H. Gies, H. Imai, T. Tatsumi, D. De Vos, *Chemcatchem*, 2011, **3**, 1442.
34. W. J. Roth, P. Nachtigall, R. E. Morris, P. S. Wheatley, V. R. Seymour, S. E. Ashbrook, P. Chlubná, L. Grajciar, M. Polozij, A. Zupal, O. Shvets, J. Čejka, *Nat. Chem.*, 2013, **5**, 628.
35. S. Zanardi, A. Alberti, G. Cruciani, A. Corma, V. Fornés, M. Brunelli, *Angew. Chem. Int. Ed.*, 2004, **43**, 4933.
36. P. Gorgojoa, D. Sieffert, C. Staudtb, C. Telleza, J. Coronasa, *J. Membrane Sci.*, 2012, **411-412**, 146.
37. A. Corma, V. Fornés, U. Díaz, *Chem. Commun.*, 2001, **47**, 2642.
38. H.-L. Zubowa, M. Schneider, E. Schreier, R. Eckelt, M. Richter, R. Fricke,

- Micropor. Mesopor. Mater.*, 2008, **109**, 317.
39. P. Gorgojo, A. Galve, S. Uriel, C. Téllez, J. Coronas, *Micropor. Mesopor. Mater.*, 2011, **142**, 122.
40. W. J. Roth, C. T. Kresge, *Micropor. Mesopor. Mater.*, 2011, **144**, 158.
41. A. Galve, P. Gorgojo, N. Navascués, C. Casado, C. Téllez, J. Coronas, *Micropor. Mesopor. Mater.*, 2011, **145**, 211.
42. J.-G. Jiang, L. Jia, B. Yang, H. Xu, P. Wu, *Chem. Mater.*, 2013, **25**, 4710.
43. L. D. Rollmann, J. L. Schlenker, S. L. Lawton, C. L. Kennedy, G. J. Kennedy, *Micropor. Mesopor. Mater.*, 2002, **53**, 179.
44. B. Marler, M. A. Camblor, H. Gies, *Micropor. Mesopor. Mater.*, 2006, **90**, 87.
45. W. Fan, P. Wu, S. Namba, T. Tatsumi, *Angew. Chem. Int. Ed.*, 2003, **116**, 238.
46. T. Ikeda, S. Kayamori, Y. Oumi, F. Mizukami, *J. Phys. Chem. C*, 2010, **114**, 3466.

## Figure Captions

**Table 1.** Textural properties of Nu-6(2), calcined ECNU-4 and Del-Nu-6 prepared with various amount of TPAOH.

**Table 2.**  $^{29}\text{Si}$  NMR chemical shifts and peak area of Nu-6(1), Nu-6(2), ECNU-4-Cal and Del-Nu-6(2.4)-Cal.

**Scheme 1.** Structural diversity of Nu-6(1) zeolite in post-treatment, including calcination (a), short-time treatment in HCl/EtOH solution (b), swelling (c), and delamination (d).

**Figure 1.** XRD patterns of Nu-6(1) (a), Nu-6(2) (b) and interlayer expanded zeolite IEZ-Nu-6(1) prepared with  $\text{Me}_2\text{Si}(\text{OEt})_2$  silylation (c) or without silane addition (d) in HCl/EtOH solution at 473 K for 24 h.

**Figure 2.** TG curves of Nu-6(1) precursor (a) and after treated with in HCl/EtOH in the absence of any silane for 15 min (b), 30 min (c), 75 min (d), 2.5 h (e), 4 h (f), 12 h (g) and 24 h (h), and the change of remaining SDA content with the treatment time (i). The scales of a - h curves correspond to the bottom and left, while those of curve i correspond to the top and right.

**Figure 3.** XRD patterns of Nu-6(1) after treated in HCl/EtOH for 15 min (a), 30 min (b), 75 min (c), 2.5 h (d), 4 h (e), 12 h (f) and 24 h (g).

**Figure 4.** XRD patterns of Nu-6(1) (a), ECNU-4 (b), ECNU-4-cal (c) and Nu-6(2) (d).

**Figure 5.** XRD patterns of swollen ECNU-4 samples (A) and Del-Nu-6 (B) with 1.5 g (a), 2.4 g (b), 2.8 g (c) and 3.6 g (d) TPAOH per gram of ECNU-4.

**Figure 6.** N<sub>2</sub> adsorption isotherms of Nu-6(2) (a), ECNU-4-Cal (b), and Del-Nu-6-Cal materials prepared with 1.5 g (c), 2.4 g (d), 2.8 g (e), and 3.6 g (f) TPAOH per gram of ECNU-4.

**Figure 7.** SEM images of Nu-6(1) (a) and ECNU-4 (b), swollen ECNU-4(2.4) (c) and Del-Nu-6(2.4)(d).

**Figure 8.** <sup>29</sup>Si MAS NMR spectra of Nu-6(1) (a), Nu-6(2) (b), ECNU-4(c) and Del-Nu-6(2.4) (d).

**Table 1.** Textural properties of Nu-6(2), calcined ECNU-4 and Del-Nu-6 prepared with various amount of TPAOH.

No.	Sample	Surface area (m <sup>2</sup> g <sup>-1</sup> )	
		Total	External ( <i>t</i> -plot)
1	Nu-6(2)	35	24
2	ECNU-4-Cal	82	45
3	Del-Nu-6(1.5)-Cal	94	69
5	Del- Nu-6(2.4)-Cal	127	87
6	Del-Nu-6(2.8)-Cal	132	60
8	Del- Nu-6(3.6)-Cal	146	61

<sup>a</sup>Calculated by BET method. <sup>b</sup> Calculated by *t*-plot method.

**Table 2.**  $^{29}\text{Si}$  NMR chemical shifts and peak area of Nu-6(1), Nu-6(2), ECNU-4-Cal and Del-Nu-6(2.4)-Cal.

Sample	$Q^3$ <sup>a</sup>	$Q^4$ <sup>a</sup>
Nu-6(1)	-103.8 (27.68)	-112.27 (17.09), -113.20 (55.22)
Nu-6(2)	-103.51 (15.71)	-109.94 (46.75), -112.99 (28.91), -115.99 (8.63)
ECNU-4-Cal	-103.16 (24.27)	-108.38 (39.07), -112.08 (24.15) -115.07 (12.46)
Del-Nu-6(2.4)-Cal	-103.91 (24.06)	-108.89 (35.36), -112.32 (28.14) -115.58 (12.44)

<sup>a</sup>The numbers in the parentheses indicate the percentage.

**Scheme 1.** Structural diversity of Nu-6(1) zeolite in post-treatment, including calcination (a), short-time treatment in HCl/EtOH solution (b), swelling (c), and delamination (d).

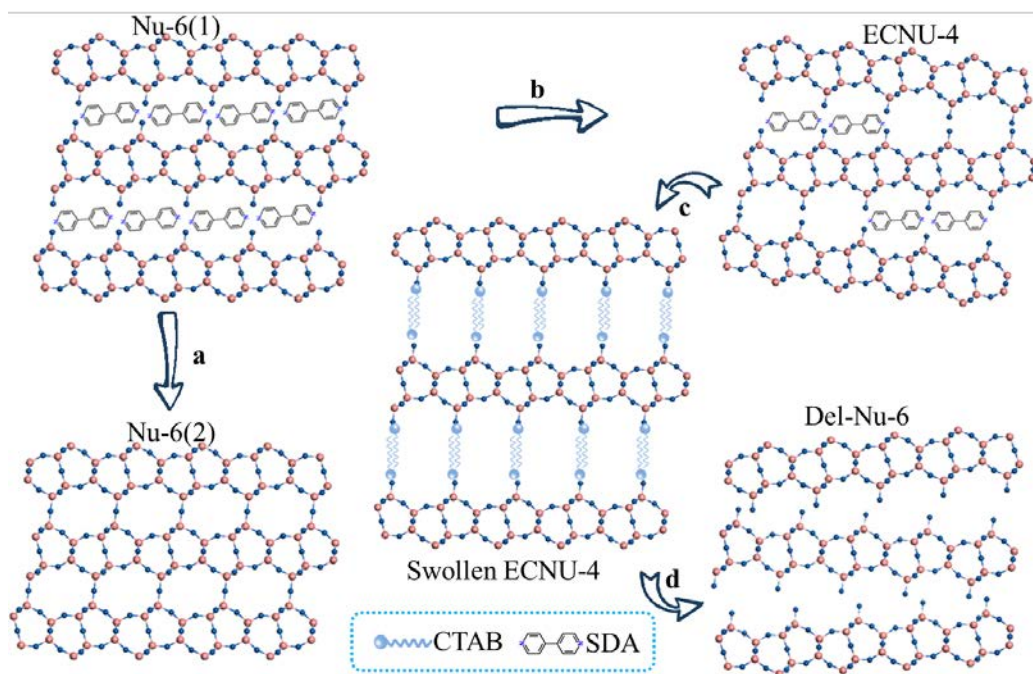


**Figure 1.** XRD patterns of Nu-6(1) (a), Nu-6(2) (b) and interlayer expanded zeolite IEZ-Nu-6(1) prepared with  $\text{Me}_2\text{Si}(\text{OEt})_2$  silylation (c) or without silane addition (d) in HCl/EtOH solution at 473K for 24 h.

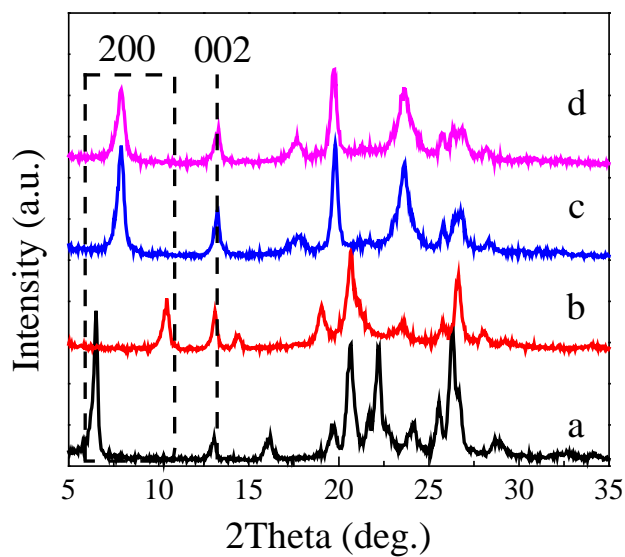


**Figure 2.** TG curves of Nu-6(1) precursor (a) and after treated with in HCl/EtOH in the absence of any silane for 15min (b), 30 min(c), 75 min (d), 2.5 h (e), 4 h (f), 12 h (g) and 24 h (h), and the change of remaining SDA content with the treatment time (i). The scales of a - h curves correspond to the bottom and left, while those of curve i correspond to the top and right.

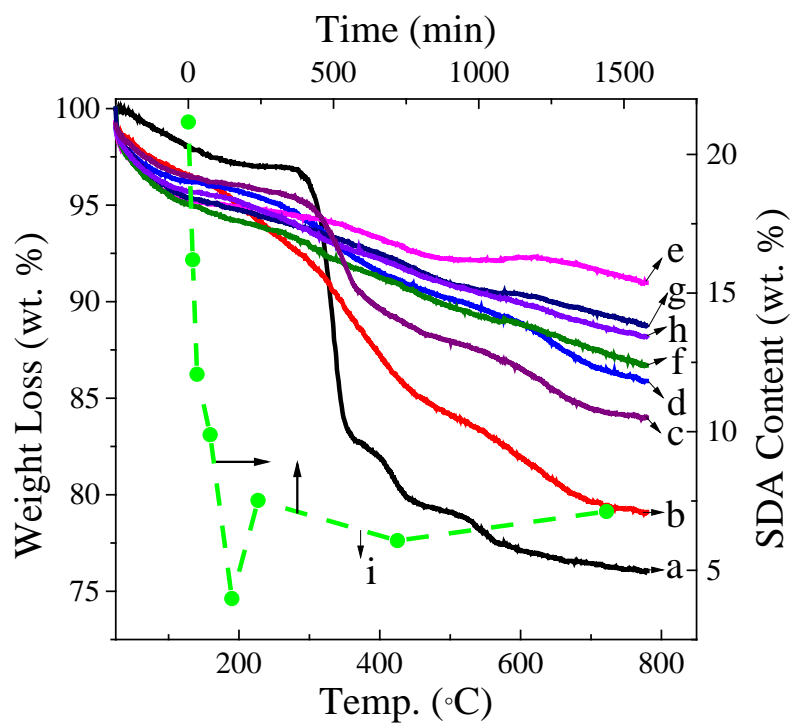


**Figure 3.** XRD patterns of Nu-6(1) after treated in HCl/EtOH for 15 min (a), 30 min (b), 75 min (c), 2.5 h (d), 4 h (e), 12 h (f) and 24 h (g).

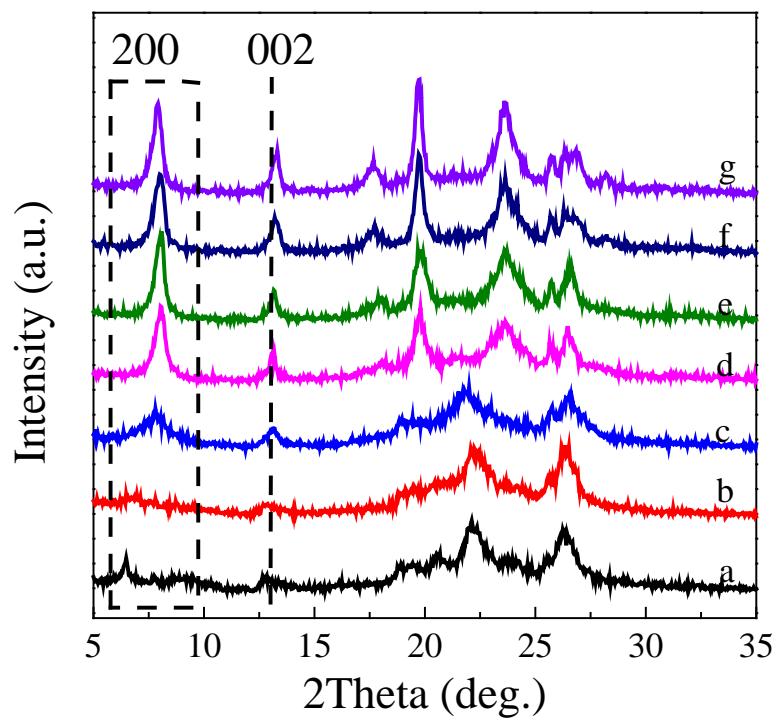


**Figure 4.** XRD patterns of Nu-6(1) (a), ECNU-4 (b), ECNU-4-cal (c) and Nu-6(2) (d).

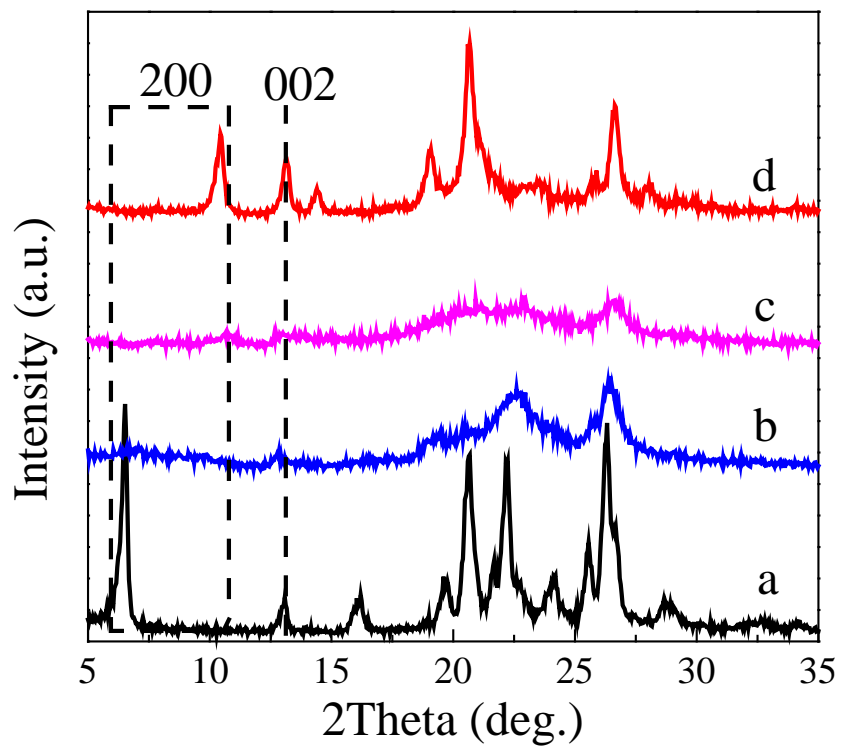


**Figure 5.** XRD patterns of swollen ECNU-4 samples (A) and Del-Nu-6 (B) with 1.5 g (a), 2.4 g (b), 2.8 g (c) and 3.6 g (d) TPAOH per gram of ECNU-4.

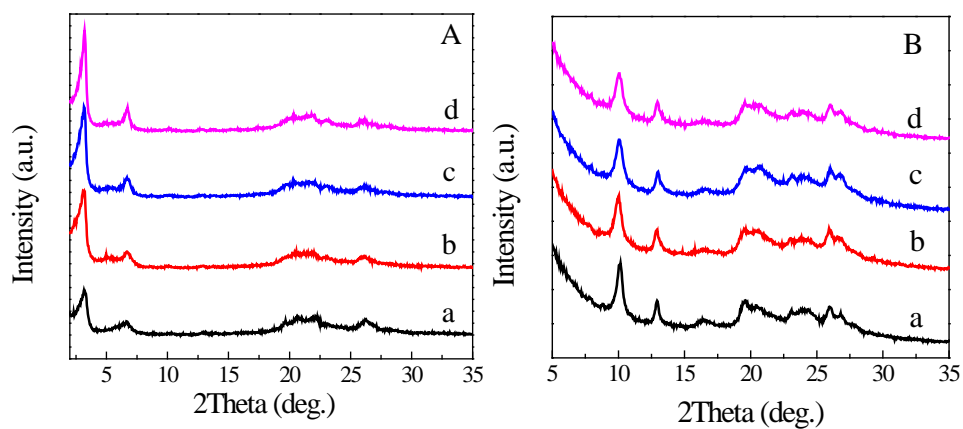


**Figure 6.** N<sub>2</sub> adsorption isotherms of Nu-6(2) (a), ECNU-4-Cal (b), and Del-Nu-6-Cal materials prepared with 1.5 g (c), 2.4 g (d), 2.8 g (e), and 3.6 g (f) TPAOH per gram of ECNU-4.

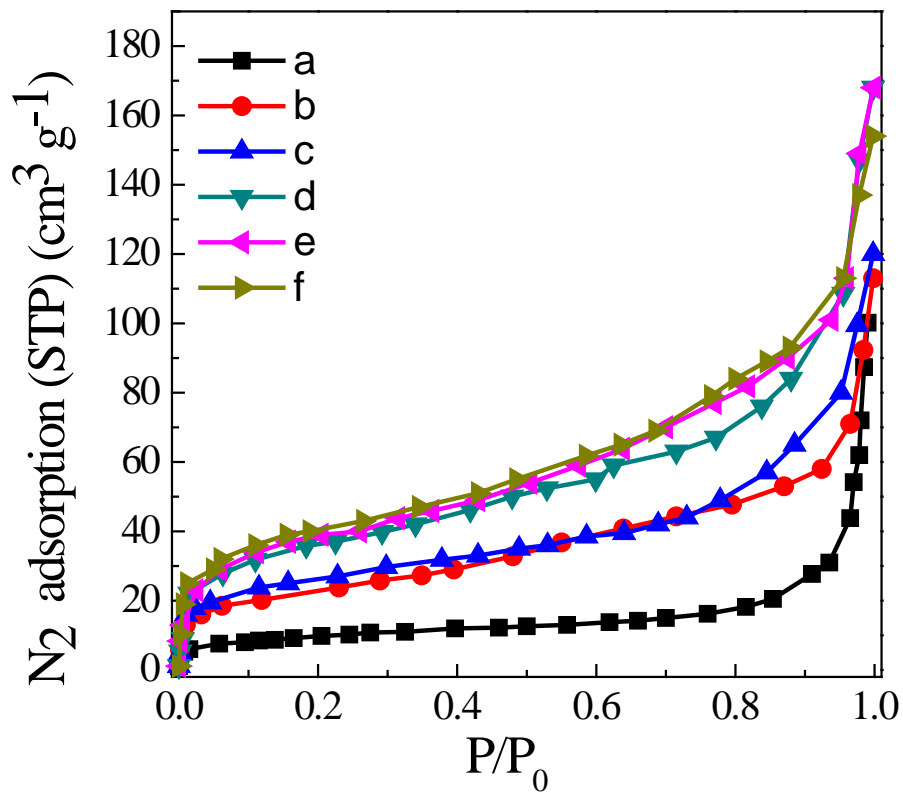


**Figure 7.** SEM images of Nu-6(1) (a) and ECNU-4 (b), swollen ECNU-4(2.4) (c) and Del-Nu-6(2.4) (d).

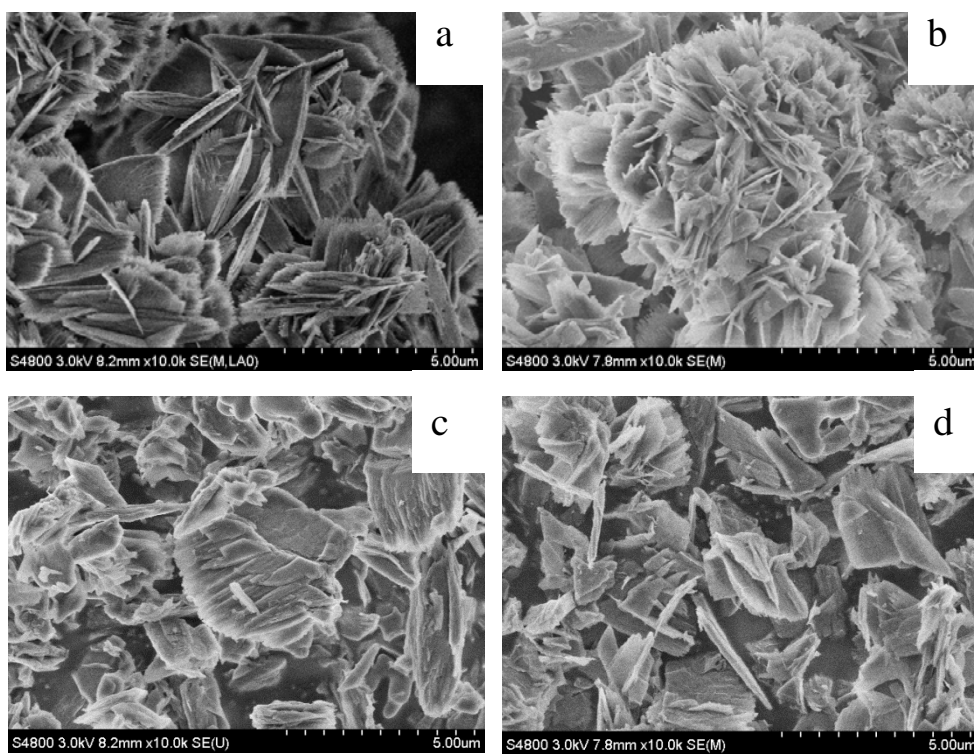


**Figure 8.**  $^{29}\text{Si}$  MAS NMR spectra of Nu-6(1) (a), Nu-6(2) (b), ECNU-4(c) and Del-Nu-6(2.4) (d).

